

Supporting Information

Three-dimensionally ordered mesoporous carbons activated by hot ammonia treatment as a high-performance anode material in lithium-ion batteries

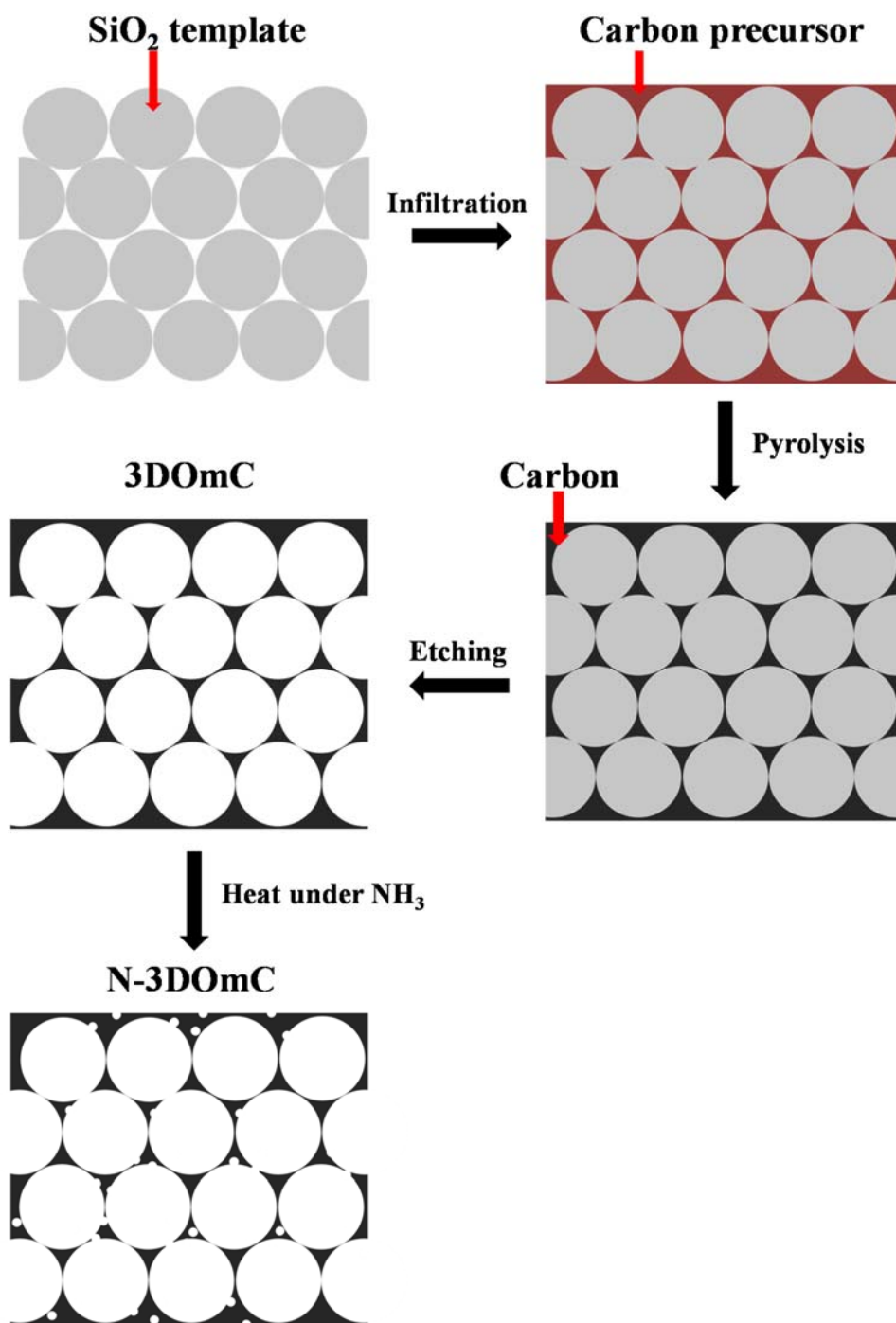
*Bin Han,^a Eun Joo Lee,^a Won Ho Choi,^a Won Cheol Yoo^{*b} and Jin Ho Bang^{*ab}*

Department of Bionanotechnology and Department of Chemistry and Applied Chemistry, Hanyang University, 55 Hanyangdaehak-ro, Sangnok-gu, Ansan, Kyeonggi-do 426-791, Republic of Korea

Email: jbang@hanyang.ac.kr (J. H. Bang), wcyoo@hanyang.ac.kr (W. C. Yoo)

^aDepartment of Bionanotechnology

^bDepartment of Chemistry and Applied Chemistry



Scheme S1 Schematic illustration of the synthesis of 3DOmCs and N-3DOmCs.

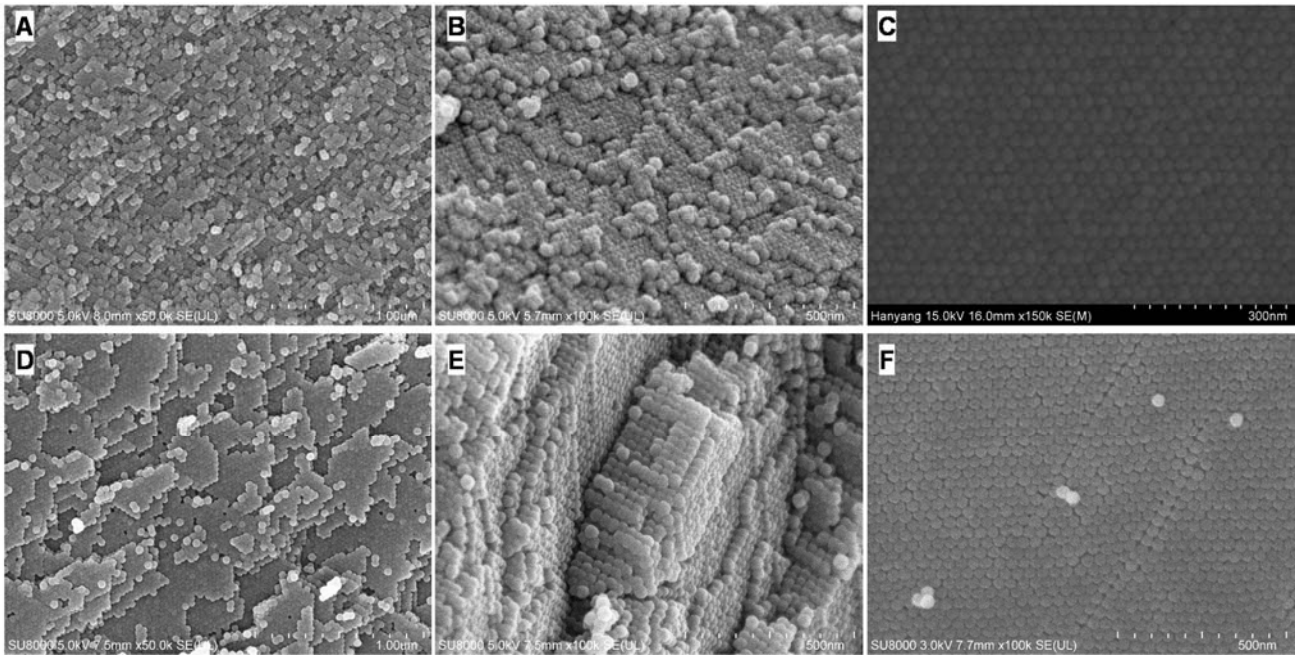


Fig. S1 SEM images of SiO₂ templates used for (A-C) 16 nm and (D-F) 32 nm 3DOMCs.

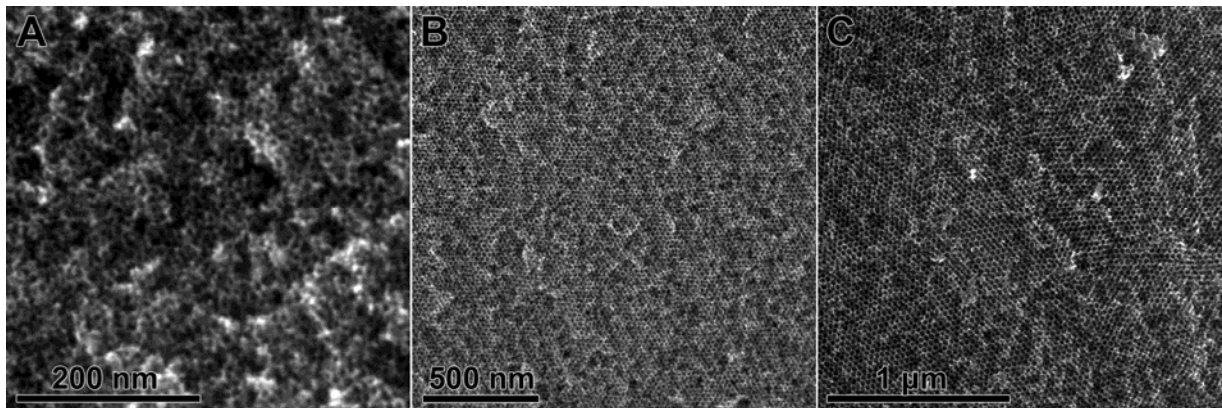


Fig. S2 Additional SEM images of 3DOMCs with pore size (A) 8 nm, (B) 16 nm, and (C) 32 nm.

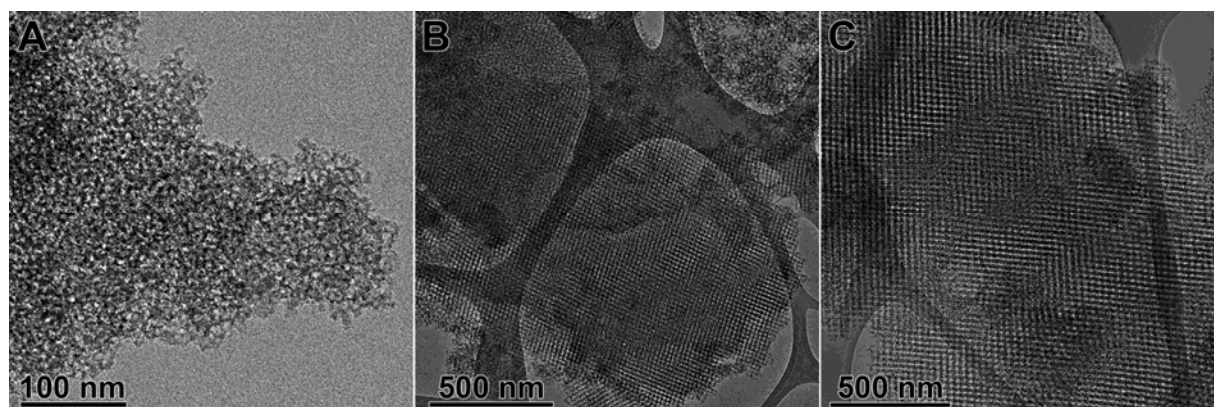


Fig. S3 Additional TEM images of 3D OmCs with pore size (A) 8 nm, (B) 16 nm, and (C) 32 nm.

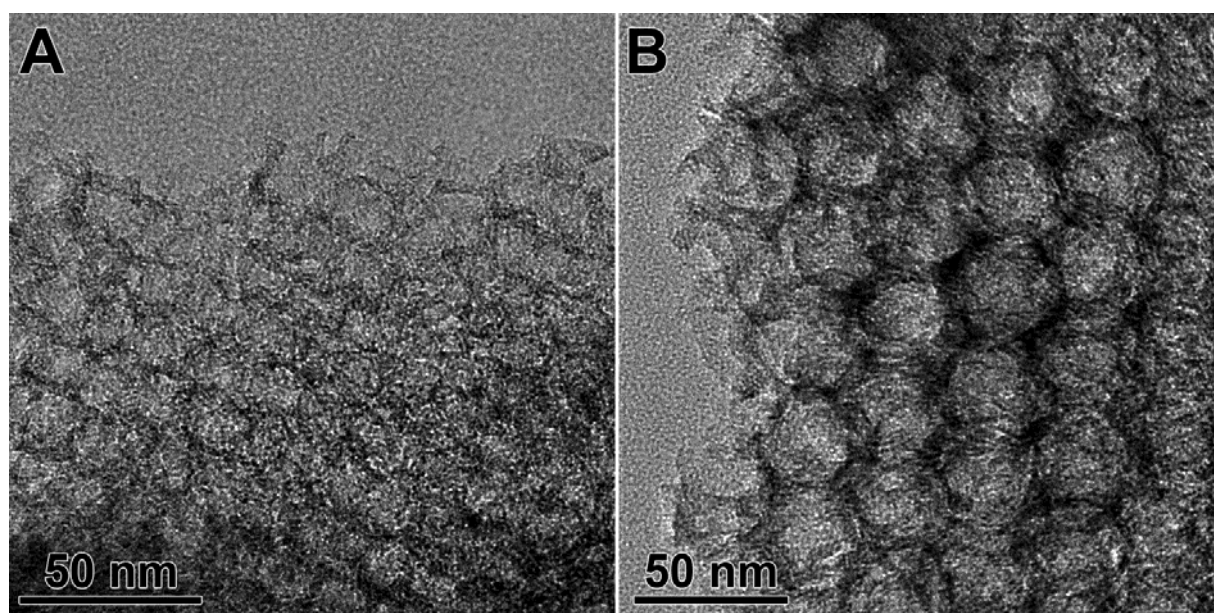


Fig. S4 Additional TEM images of N-3D OmCs with pore size (A) 16 nm and (B) 32 nm.

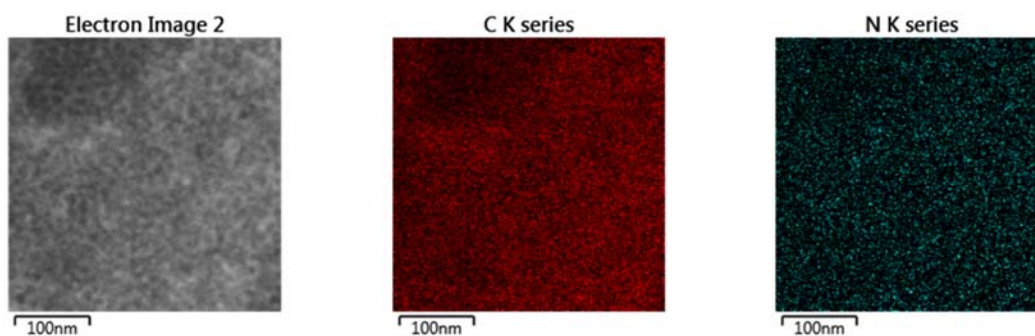
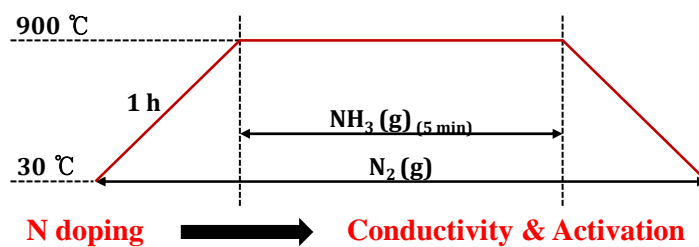


Fig. S5 TEM-EDS mapping analysis of 16nm_N-3DOmC.



Scheme S2 Schematic illustration of NH_3 heat treatment of 3DOmCs for the fabrication of N-3DOmCs.

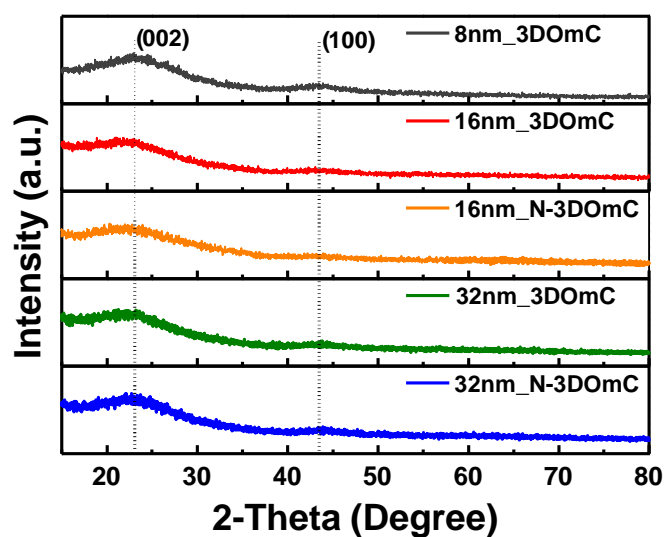


Fig. S6 XRD patterns of 3DOmCs and N-3DOmCs.

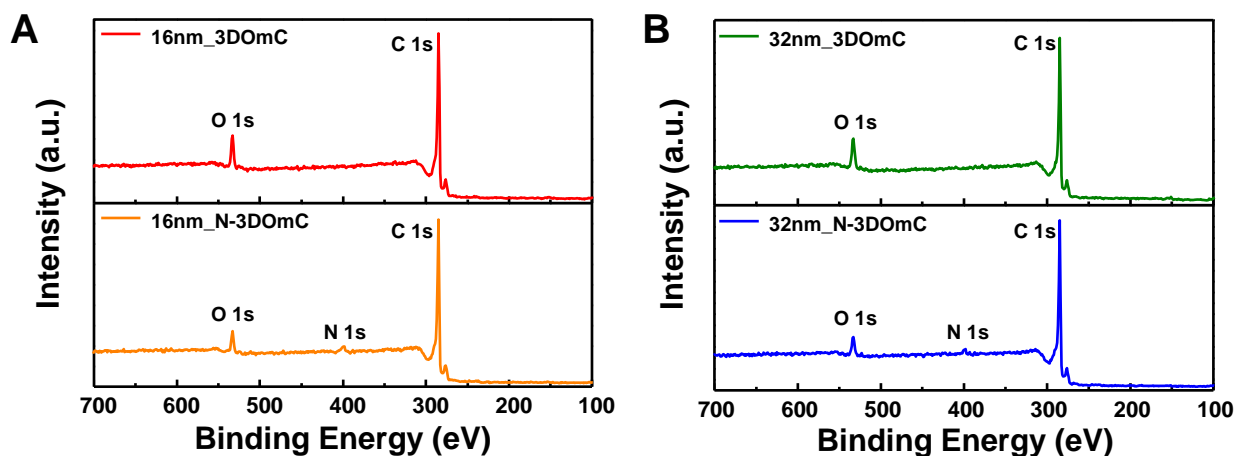


Fig. S7 XPS spectra of (A) 16nm_3DOmCs and (B) 32nm_3DOmCs before and after NH_3 heat treatment.

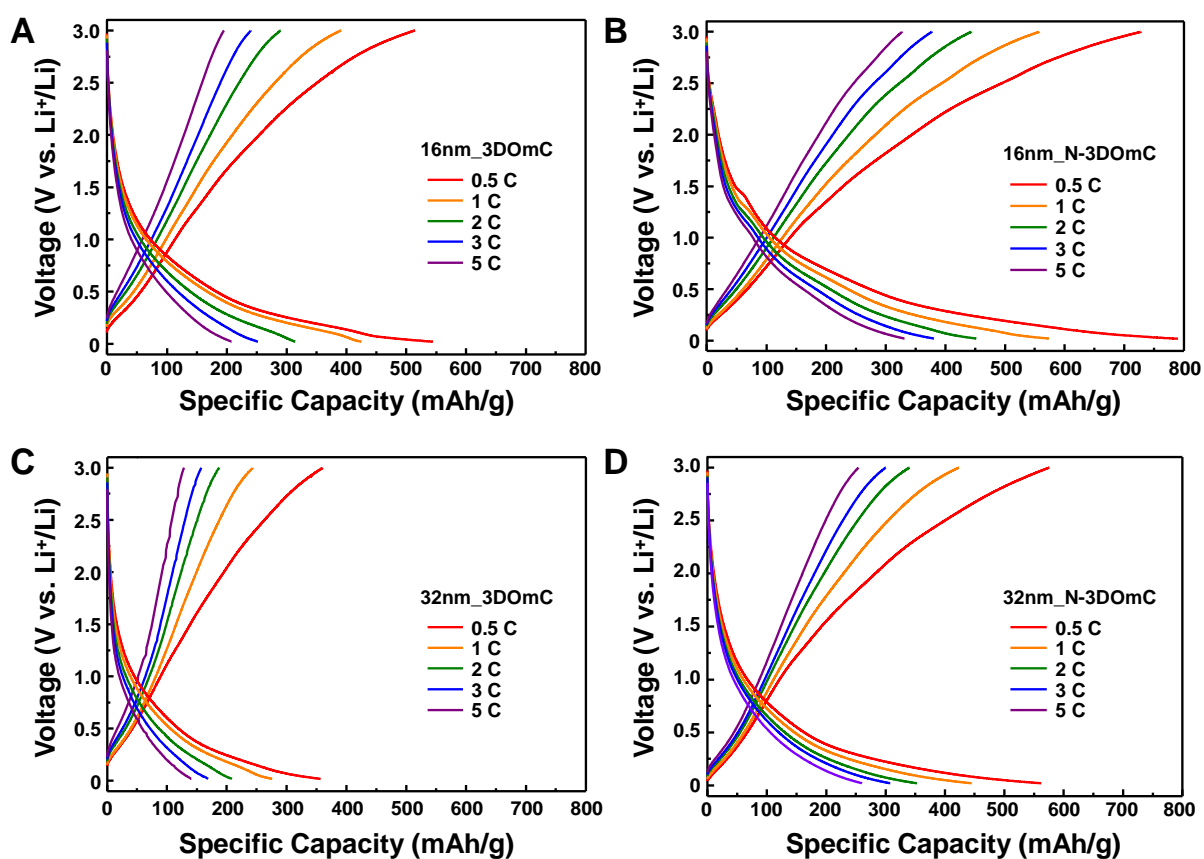


Fig. S8 Charge/discharge curves of (A) 16nm_3DOmC, (B) 16nm_N-3DOmC, (C) 32nm_3DOmC, and (D) 32nm_N-3DOmC anodes at various C-rates.

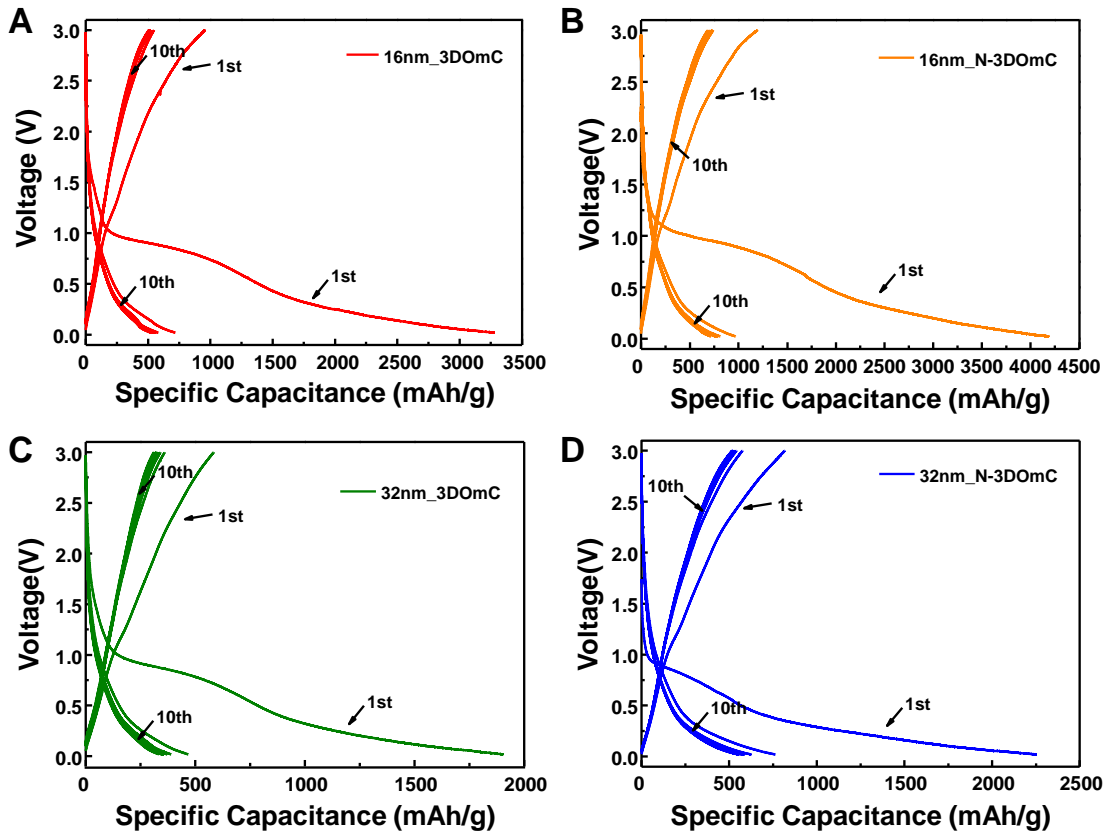


Fig. S9 Initial charge/discharge curves of A) 16nm_3DOmC, (B) 16nm_N-3DOmC, (C) 32nm_3DOmC, and (D) 32nm_N-3DOmC anodes. Note that the 1st cycle was recorded at 0.1 C, whereas 2nd~10th cycles at 0.5 C.

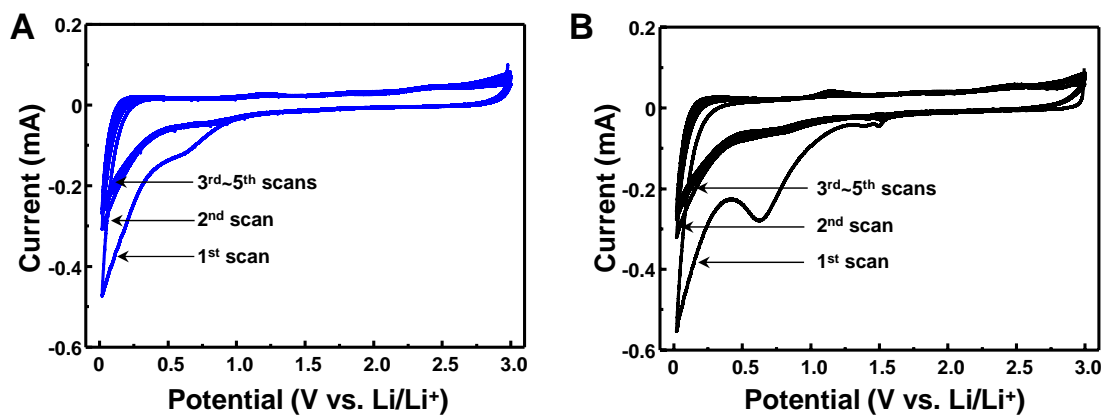


Fig. S10 Cyclic voltammograms of (A) 16nm_3DOmC and (B) 16nm_N-3DOmC at a scan rate of 0.1 mV/s.

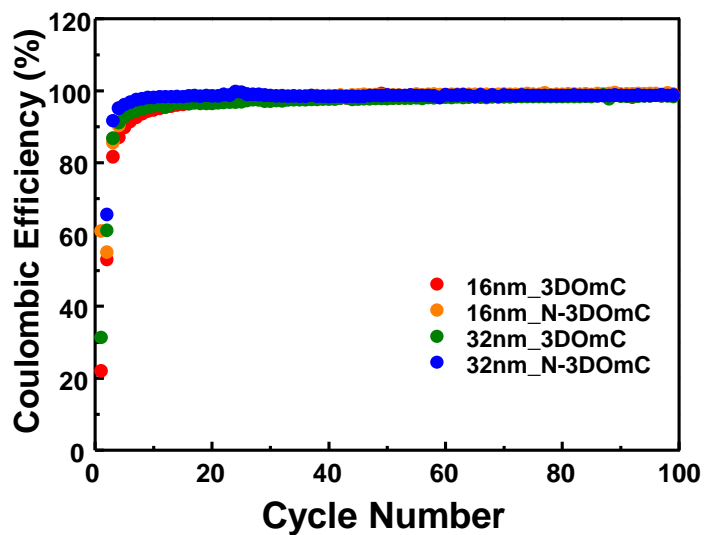


Fig. S11 Coulombic efficiency of 3DOmCs and N-3DOmCs.

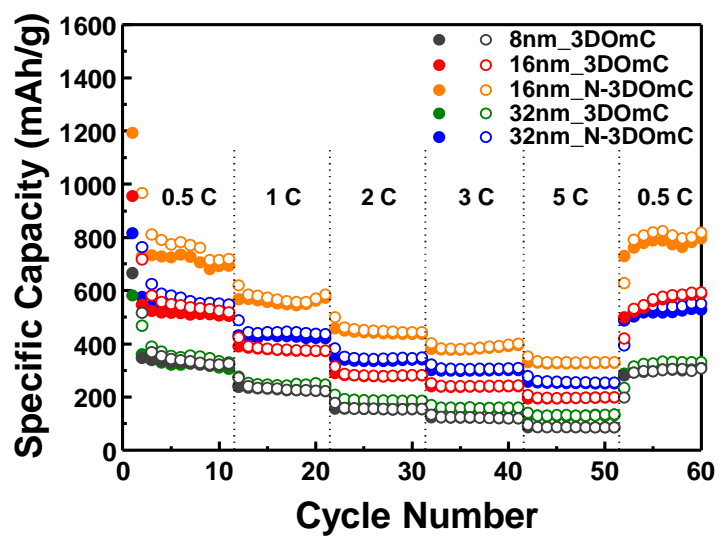


Fig. S12 Specific capacities of 3DOmCs and N-3DOmCs cycled at various C-rates.

Table S1. Voltage measurements of 16nm_3DOmC and 16nm_N-3DOmC at a given current (0.01 mA), which reflect the electrical conductivity of these carbons. Since $R=V/I$, the larger voltages, the higher resistances (also higher resistivity).

Trial at 0.01 mA	3DOmC	N-3DOmC
1	1.6 V	0.38 V
2	1.4 V	0.8 V
3	1.3 V	1.2 V
4	1.5 V	0.5 V
5	1.5 V	0.4 V
6	1.4 V	1.2 V
Average	1.45 V	0.75 V

Calculation of density of 3DOmC materials:

- Assumption,

1. The density of solid carbon is assumed to be 2 g/cc (usually 1.8–2.1 g/cc).
2. The silica particles are packed as face-centered cubic array (packing density = 74 %).
3. The size of silica sphere is assumed to be uniform.
4. The density of air at 25 °C is 0.00118 g/cc.
5. The pores of 3DOmCs consist of mesopores and micropores, and the information of pore volumes of both pores is determined by nitrogen-sorption measurements.

Then, the 3DOmC has 74 % free volume filled with air at ambient condition, because it is the inverse structure of the closed packed silica templates. → 26 % of carbon for 3DOmC sample

So the density of 3DOmC without considering microporosity is

$$(0.26 \times 2 \text{ g/cc}) + (0.74 \times 0.00118 \text{ g/cc}) = 0.52 \text{ g/cc}$$

Then, the microporosity of the 3DOmC samples now is needed to be considered as follows:

For example, 32nm_N-3DOmC has 0.169 cc/g of microporosity, then, the emptiness inside 32nm_N-3DOmC is 33.8 % (carbon fraction is then 66.2 %).

When considering the microporosity for 32nm_N-3DOmC, the calculated density is

$$\therefore (0.26 \times 0.662 \times 2 \text{ g/cc}) + (0.26 \times 0.338 \times 0.00118 \text{ g/cc}) + (0.74 \times 0.00118 \text{ g/cc}) = 0.345 \text{ g/cc}$$